

AFWAL-TR-83-3084, Vol. II



AD A139241

**FATIGUE DAMAGE - STRENGTH
RELATIONSHIPS IN COMPOSITE
LAMINATES
VOL II**

K. L. Reifsnider and W. W. Stinchcomb

Materials Response Group
Engineering Science and Mechanics Department
Virginia Polytechnic Institute and State University
Blacksburg, VA 24061-4899

15 January 1984

Final Report For Period December 1982 - April 1983

APPROVED FOR PUBLIC RELEASE; DISTRIBUTION UNLIMITED

DTIC
ELECTE
MAR 22 1984
S B

DTIC FILE COPY

FLIGHT DYNAMICS LABORATORY
AIR FORCE WRIGHT AERONAUTICAL LABORATORIES
AIR FORCE SYSTEMS COMMAND
WRIGHT-PATTERSON AIR FORCE BASE, OHIO 45433


84 03 22 005

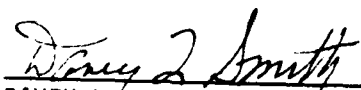
NOTICE

When Government drawings, specifications, or other data are used for any purpose other than in connection with a definitely related Government procurement operation, the United States Government thereby incurs no responsibility nor any obligation whatsoever; and the fact that the government may have formulated, furnished, or in any way supplied the said drawings, specifications, or other data, is not to be regarded by implication or otherwise as in any manner licensing the holder or any other person or corporation, or conveying any rights or permission to manufacture use, or sell any patented invention that may in any way be related thereto.

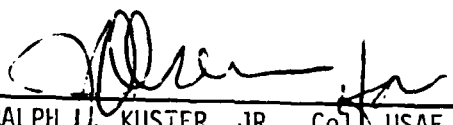
This report has been reviewed by the Office of Public Affairs (ASD/PA) and is releasable to the National Technical Information Service (NTIS). At NTIS, it will be available to the general public, including foreign nations.

This technical report has been reviewed and is approved for publication.


GEORGE P. SENDECKY, Aero. Engr.
Fatigue, Fracture & Reliability Gp.
Structural Integrity Branch
Structures & Dynamics Division


DAVEY L. SMITH, Chief
Structural Integrity Branch
Structures & Dynamics Division

FOR THE COMMANDER:


RALPH L. KUSTER, JR., COL USAF
Chief, Structures & Dynamics Division

"If your address has changed, if you wish to be removed from our mailing list, or if the addressee is no longer employed by your organization please notify AFWAL/FIBE, W-P AFB, OH 45433 to help us maintain a current mailing list".

Copies of this report should not be returned unless return is required by security considerations, contractual obligations, or notice on a specific document.

Unclassified

SECURITY CLASSIFICATION OF THIS PAGE

REPORT DOCUMENTATION PAGE				
1a. REPORT SECURITY CLASSIFICATION Unclassified		1b. RESTRICTIVE MARKINGS		
2a. SECURITY CLASSIFICATION AUTHORITY		3. DISTRIBUTION/AVAILABILITY OF REPORT Approved for public release; distribution unlimited.		
2b. DECLASSIFICATION/DOWNGRADING SCHEDULE				
4. PERFORMING ORGANIZATION REPORT NUMBER(S)		5. MONITORING ORGANIZATION REPORT NUMBER(S) AFWAL-TR-83-3084, Vol. II		
6a. NAME OF PERFORMING ORGANIZATION Virginia Polytechnic Institute & State University		6b. OFFICE SYMBOL (If applicable)		7a. NAME OF MONITORING ORGANIZATION Flight Dynamics Laboratory (AFWAL/FIBE) Air Force Wright Aeronautical Laboratories
6c. ADDRESS (City, State and ZIP Code) Blacksburg, VA 24061		7b. ADDRESS (City, State and ZIP Code) Wright Patterson AFB, OH 45433		
8a. NAME OF FUNDING/SPONSORING ORGANIZATION		8b. OFFICE SYMBOL (If applicable)		9. PROCUREMENT INSTRUMENT IDENTIFICATION NUMBER F33615-81-K-3225
8c. ADDRESS (City, State and ZIP Code)		10. SOURCE OF FUNDING NOS.		
		PROGRAM ELEMENT NO. 61102F	PROJECT NO. 2307	TASK NO. N1 WORK UNIT NO. 17
11. TITLE (Include Security Classification) FATIGUE DAMAGE - STRENGTH RELATIONSHIPS IN COMPOSITE LAMINATES				
12. PERSONAL AUTHOR(S) K.L. Reifsnider and W.W. Stinchcomb				
13a. TYPE OF REPORT Final		13b. TIME COVERED FROM Dec 82 TO Apr 83		14. DATE OF REPORT (Yr., Mo., Day) 84 Jan 15
15. PAGE COUNT 62				
16. SUPPLEMENTARY NOTATION				
17. COSATI CODES			18. SUBJECT TERMS (Continue on reverse if necessary and identify by block number)	
FIELD	GROUP	SUB. GR.	composite materials, fatigue, damage, stiffness change, delamination, matrix cracks, fiber fracture, NDE	
11	04			
01	03			
19. ABSTRACT (Continue on reverse if necessary and identify by block number) This report presents information and experience generated during the subject investigation which provided support for the major thrust of the effort, but was not the eventual focus of the program. The activities are discussed in the context of the various experimental techniques used (and developed) to investigate fracture-related damage development. While much of the information discussed is not complete, it is thought that a description of the experimental methods and experiences will be valuable to the technical community. Included are descriptions of virtually every experimental technique used in this program and a variety of findings not discussed elsewhere.				
20. DISTRIBUTION/AVAILABILITY OF ABSTRACT UNCLASSIFIED/UNLIMITED <input checked="" type="checkbox"/> SAME AS RPT. <input type="checkbox"/> DTIC USERS <input type="checkbox"/>			21. ABSTRACT SECURITY CLASSIFICATION Unclassified	
22a. NAME OF RESPONSIBLE INDIVIDUAL GEORGE P. SENDECKYJ			22b. TELEPHONE NUMBER (Include Area Code) (513) 255-6104	22c. OFFICE SYMBOL AFWAL/FIBEC

PREFACE

The work reported herein was performed under Contract F33615-81-K-3225, Project 2307, Work Unit 2307N117, sponsored by the Flight Dynamics Laboratory of the Air Force Wright Aeronautical Laboratories, Wright Patterson AFB, Ohio 45433. Dr. G.P. Sendeckyj, AFWAL/FIBE, was the Air Force Project Monitor.

The authors express their appreciation to the Air Force for their support of this program; to George Sendeckyj for his help, encouragement, and guidance; to G.K. McCauley for his assistance with the photo and art work; and to Mrs. Barbara Wengert for typing the manuscript.

Accession For		<input checked="checked" type="checkbox"/>
NTIS GRA&I		<input checked="checked" type="checkbox"/>
DTIC TAB		<input type="checkbox"/>
Unannounced		<input type="checkbox"/>
Justification		
By		
Distribution/		
Availability Codes		
Dist	Avail and/or Special	
A-1		

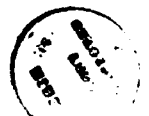


TABLE OF CONTENTS

	<u>Page</u>
INTRODUCTION	1
DAMAGE AND MATERIAL RESPONSE	3
DAMAGE MEASUREMENT USING ESTABLISHED METHODS	4
DAMAGE MEASUREMENT USING RECENTLY DEVELOPED METHODS	12
FIBER FRACTURE	37
REFERENCES	47

LIST OF ILLUSTRATIONS

<u>Figure</u>	<u>Page</u>
<p>1. Edge Replicas of a Progressively Fatigue-Damaged $[0,90_2]_S$ Laminate, $\sigma_{\max}/\sigma_{\text{ult}} = 0.70$:</p> <p style="margin-left: 20px;">a) 1 cycle, Stage I;</p> <p style="margin-left: 20px;">b) 1400 cycles, 1 percent stiffness change, Stage I;</p> <p style="margin-left: 20px;">c) 22,000 cycles, 3 percent stiffness change, Stage II.</p>	6
<p>2. X-ray Radiographs of Fatigue-Damaged Laminates:</p> <p style="margin-left: 20px;">a) $[0,90_2]_S$, $\sigma_{\max}/\sigma_{\text{ult}} = 0.70$, 26,000 cycles, 3 percent change in stiffness, Stage II;</p> <p style="margin-left: 20px;">b) $[0,90,\pm 45]_S$, $\sigma_{\max}/\sigma_{\text{ult}} = 0.62$, 78,000 cycles, 18 percent stiffness change, Stage III</p>	8
<p>3. Transverse section of a $[0,90_2]_S$ Laminate Showing Longitudinal Matrix Crack in Zero Deg Ply and Delamination on 0/90 Interface: $\sigma_{\max}/\sigma_{\text{ult}} = 0.70$, Stage III</p>	10
<p>4. Experimental arrangement for stress wave factor measurements.</p>	14
<p>5. Stress wave factor data compared to failure location (shaded) for a glass-epoxy specimen.</p>	16
<p>6. Comparison of stress wave factor measurements with local stiffness implied from a moiré diffraction pattern.</p>	18
<p>7. Comparison of changes in SWF and axial stiffness of a fatigue loaded laminated composite specimen.</p>	20
<p>8. Correlation of several types of nondestructive test data for a fatigue loaded $[0,90_2]_S$ glass-epoxy specimen.</p>	22
<p>9. Residual strength (open circles) and stiffness changes (dotted line) for a series of fatigue tests on glass-epoxy specimens.</p>	24
<p>10. Schematic of experimental arrangement for moiré diffraction investigations.</p>	27

11.	Moiré diffraction pattern showing local increased strains in 0 deg. plies due to cracks in 90 deg. plies of a $[0,90_3]_5$ glass-epoxy specimen.	29
12.	Method of construction of controlled regions of delamination for stress redistribution studies.	30
13.	Moiré fringe pattern taken from specimen SC-1 spalling both undamaged and delaminated regions.	32
14.	Comparison of specimen effective stiffness in delaminated and undelaminated regions.	35
15.	Average number of fibers broken in a fixed area of viewing at about one-third, two-thirds, and nearly one full lifetime of cyclic loading for a graphite epoxy laminate.	40
16.	Total fiber fractures in $[0,90,\pm 45]_5$ laminates.	41

LIST OF TABLES

- I. Comparison of in-plane stresses predicted via laminate analysis for a $[0,90,90,0,+45,-45,-45,+45]_s$ graphite epoxy laminate (lamina properties: $E_1 = 141.6$ GPa, $E_2 = 10.2$ GPa, $\nu_{12} = 0.305$, $G_{12} = 6.00$ GPa, $N_x = 113.0$ kN-mm) with and without delamination at the 0-45 interfaces. 34

INTRODUCTION

While phenomenological characterization is always required when questions of strength or life must be answered, the ultimate accuracy and success of engineering models of behavior depends greatly on the degree to which they are based on an understanding of the mechanisms which produce damage and reduce the strength and life of engineering components. This is especially true if predictions of behavior are to be made for situations for which no experience is available. It is also important to understand damage mechanisms if improvements in material design and optimization of component design are to be attempted.

The present research effort is concerned with the identification, characterization, and analysis of damage events and mechanisms associated with low-amplitude fatigue loading of graphite epoxy laminates for large numbers of cycles, such that the strength, stiffness and life of the laminates are reduced significantly. In particular, this investigation has focused on the precise manner in which those damage events and mechanisms produce a state of stress and state of material which induces the ultimate fracture of such fatigue-loaded composite laminates. A systematic and comprehensive study of damage development throughout the life of such specimens was attempted in the present case, and several unique experimental techniques were used to obtain valuable new information about the precise nature of the micro-events. Several different laminate types and two different materials were used in an effort to identify features which are generic to damage development in laminates under this type of loading. A detailed description of many of the results obtained was presented in Vol. I of

this report. However, the scope of that document was constrained to a group of investigative activities which were closely associated and which eventually became the backbone of the new philosophies and results generated in this effort. The present report will deal with two additional aspects of our work. First, a thorough discussion of the experimental methods which were used (and some developed) to investigate various fracture-related damage development events and activities will be presented and will be the basis of the "story line" of this report. Second, the report will present information and experience generated during the investigation which provided support for the major thrust of the effort but was not the eventual focus of the program. Much of that information is very valuable in the opinion of the investigators, but is frequently incomplete and raises questions which are yet unanswered.

DAMAGE AND MATERIAL RESPONSE

Studies of damage-material response relationships must include carefully designed and developed destructive and nondestructive investigative methods. The goal of these studies is to determine how the progressive development of damage throughout the loading history changes properties such as strength, stiffness, and life of composite laminates. When possible, the experiments should be designed to permit the nondestructive measurement of damage on the same specimens used to measure strength and stiffness or life and stiffness. This approach provides a description of the damage and a measurement of the consequences of the damage on response for a given loading history [1].

Although no single destructive or nondestructive inspection method is capable of detecting all damage modes in a composite laminate [2], many of the major components of the damage state can be determined using a carefully selected array of methods. Some damage detection methods are well established and are in general use in damage studies. Other techniques are more specialized, and in some cases, recently developed for or applied to composite laminates. The list of established methods used in the present program consists of stiffness monitoring, X-ray radiography, replication, and sectioning. Recently developed and applied techniques include the stress wave factor, moiré interferometry, and deply/microscopy. Details of the use of the established methods and the results are given in Ref. [3] and are summarized here. A more complete description of the recent methods and applications is presented in this report.

DAMAGE MEASUREMENT USING ESTABLISHED METHODS

Under increasing monotonic tensile loads and cyclic tensile loads, the $[0,90_2]_s$, $[0,\pm45]_s$, and $[0,90\pm45]_s$ graphite epoxy laminates develop matrix cracks in the off-axis plies. The matrix cracks cause a small decrease in the stiffness of the laminate. The stiffness reduction throughout the loading history was monitored in real-time using a Z-80 microprocessor based data acquisition system. As additional matrix cracks form and other modes of damage develop, the stiffness of the laminates continues to decrease. The stiffness change vs. cycles curve for each of the three laminates studied in this investigation showed three distinct stages of stiffness reduction. For a given type of laminate, damage rates were characterized by the rate of stiffness degradation (stages I, II, and III) due to the collective effect of the damage modes in the laminates.

Matrix cracks were detected along the edge of the specimens using the replication technique whereby a strip of cellulose-acetate tape is softened with acetone and pressed along the polished edge of the specimens. When the tape dries and hardens, an impression of the topography of the entire surface is permanently recorded on the tape. It is important to make the replicas while the specimens are under load so that the damage on the edge of the specimens is open and more readily discernible. A small tensile load (500-1000 lbs) is usually sufficient to open matrix cracks in most laminates, although it is suggested that the load not exceed the mean tensile load used in the cyclic loading histories. The picture of damage can be viewed through a microscope or microfiche reader and can be printed on photographic paper by

substituting the replica for a negative in a photographic enlarger. Replicas made at selected load or cycle intervals can be compared to determine the chronology of events in the edge damage process.

As the density of cracks increases, the cracks couple along the ply interfaces to initiate delaminations. The process of crack coupling, and the subsequent process of delamination growth along the edge of the specimen can be easily followed using the replication technique, Fig. 1. These processes cause additional stiffness reduction which, when monitored in real-time, provides a convenient damage analogue.

The replication technique is most often used to record matrix cracks, crack coupling, and delaminations along the edge of laminates and along interior transverse and longitudinal planes exposed by sectioning the laminates. Much finer details of damage are also contained on a replica and can be observed using a scanning electron microscope. Schulte and Stinchcomb [4] observed fractures of zero deg graphite fibers along the edge of $[0,90,0,90]_{2s}$ and $[0,\pm45,0]_{2s}$ laminates which had been subjected to monotonic and cyclic loading conditions. Fiber fractures were located near the transverse cracks in the adjacent off-axis plies and were regularly distributed with equidistant crack locations along the length of the laminates.

The replica technique requires very little time (2-3 minutes), is inexpensive, is easy to use, and provides a permanent record of damage. However, only exposed surfaces (free edges or sectioned surfaces) can be replicated. X-radiography, using an enhancing agent, was used to record the distribution of damage through the width of the laminates. Because graphite epoxy composites have a low absorptivity of X-radiation, it is necessary to infiltrate the damage regions with an

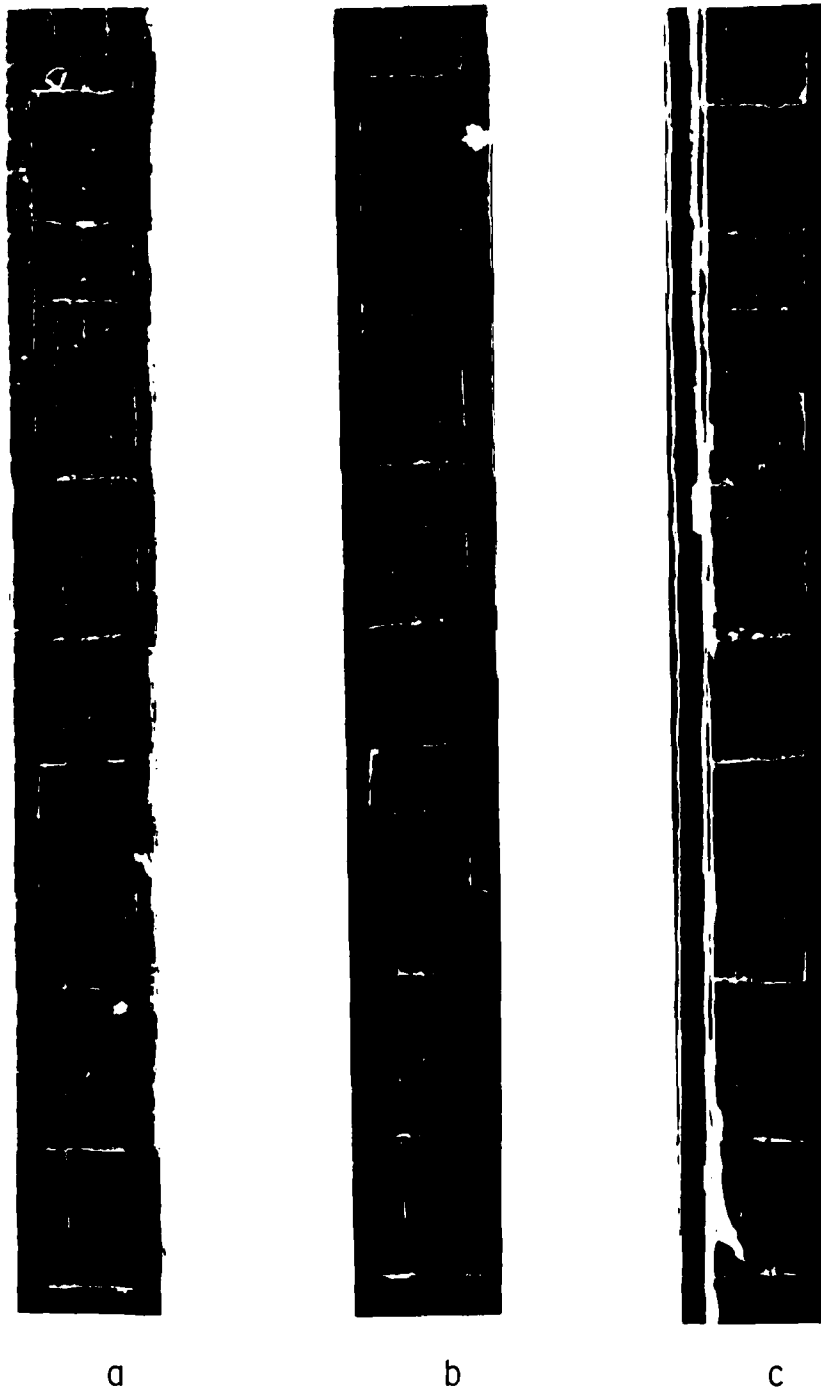


Fig. 1. Edge Replicas of a Progressively Fatigue-Damaged $[0,90_2]_s$ Laminate, $\sigma_{\max}/\sigma_{\text{ult}} = 0.70$: a) 1 cycle, Stage I; b) 1400 cycles, 1 percent stiffness change, Stage I; c) 22,000 cycles, 3 percent stiffness change, Stage II.

agent which is opaque to X-radiation. A zinc iodide solution was used as the enhancing agent in the present study. Infiltration of this agent into the specimen was aided by applying the medium to the edge of the specimen while it was positioned horizontally and subjected to a tensile load to open the cracks and delaminations. Since the accuracy of damage pictures provided by the enhanced X-ray technique depends on the degree to which the agent penetrates the damage regions, the agent must be allowed to diffuse through the specimen for some time (up to 30 min). The radiograph is then made by exposing X-ray sensitive film to a low power X-ray beam passing through the specimen. A two-dimensional X-ray of stage II fatigue damage in a $[0,90_2]_S$ laminate shows matrix cracks in the zero and 90 deg plies and small, internal delaminations at the crack intersections, Fig. 2(a). An X-ray of a $[0,90,\pm 45]_S$ laminate, Fig. 2(b), shows matrix cracks in off-axis plies and edge delamination.

X-ray radiographs, such as those in Fig. 2, present a two-dimensional view of a three-dimensional damage field. Without additional information, or insight, it is not possible to determine the interfaces which have delaminated in Fig. 2b. Because the $[0,90]_{2S}$ laminate is not geometrically complex, it is easy to infer that the small delaminations shown in Fig. 2(a) are on the 0/90 interface. A three-dimensional image of the damage field can be constructed using stereo X-ray techniques. Two radiographs of the specimen are made at different orientations to the incident X-ray beam. When the two radiographs are viewed simultaneously through a stereoscope, the relative misorientation of the two radiographs gives a perception of depth to create a three-dimensional image. Using this technique, it is possible to resolve details of damage in the direction perpendicular to



a



b

Fig. 2. X-ray Radiographs of Fatigue-Damaged Laminates: a) $[0,90_2]_s$, $\sigma_{\max}/\sigma_{\text{ult}} = 0.70$, 26,000 cycles, 3 percent change in stiffness, Stage II; b) $[0,90,+45]_s$, $\sigma_{\max}/\sigma_{\text{ult}} = 0.62$, 78,000 cycles, 18 percent stiffness change, Stage III.

the plane of the laminate. For example, the delaminations shown in Fig. 2(b) were stereoptically determined to be on 90/+45 and +45/-45 interfaces.

Additional information on the nature of the matrix cracks in zero deg plies and the internal delaminations was obtained by sectioning specimens perpendicular to and parallel to the loading axis. The sectioned surfaces were polished and examined using light and scanning electron microscopy.

The growth of stage II matrix cracks parallel to zero deg fibers in $[0,90_2]_s$ laminates is dependent on cyclic loading, a distinct contrast to the nearly simultaneous initiation and across the width growth of matrix cracks in 90 deg plies during stage I damage. The intersection of matrix cracks in adjacent zero and 90 deg plies is a point of nucleation for internal delaminations in the $[0,90_2]_s$ laminates, as shown in the radiograph of Fig. 2(a). A scanning electron micrograph of a transverse section of this laminate shows the intersecting matrix cracks in the zero and 90 deg plies and the associated internal delamination, Fig. 3. Stage III damage in the $[0,90_2]_s$ laminate is marked by an increase in the density of cracks in the zero deg plies to a saturation value and coalescence of internal delaminations. The regions of the zero deg ply isolated by the matrix cracks and the delaminations contain fewer fiber breaks than those regions of the zero degree plies which remain bonded to the 90 deg plies and contain equally spaced bands of broken fibers adjacent to the cracks in the 90 deg plies.

When used in concert, the more common methods of damage investigation provided a very detailed and complete description of

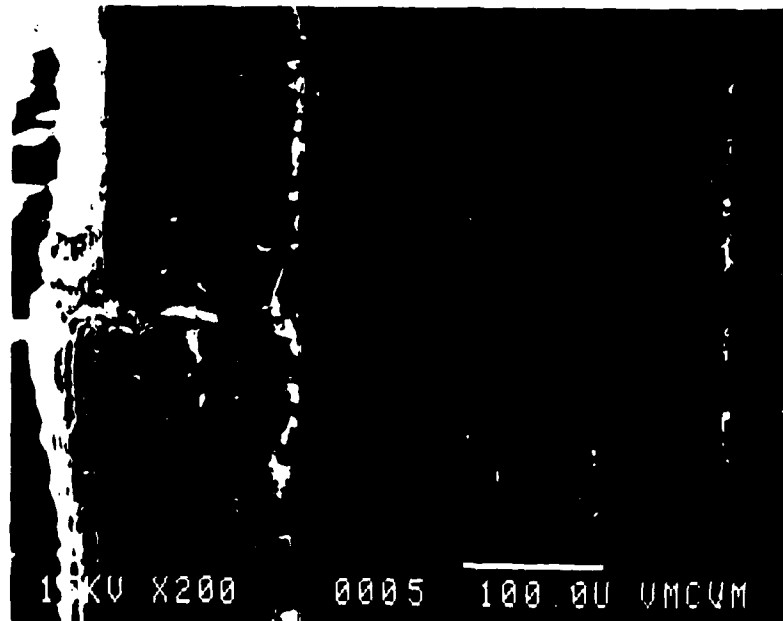


Fig. 3. Transverse Section of a $[0,90_2]_s$ Laminate Showing Longitudinal Matrix Crack in Zero Deg Ply and Delamination on 0/90 Interface: $\sigma_{\max}/\sigma_{\text{ult}} = 0.70$, Stage III.

matrix cracking and delamination in the composite laminates. The collective effect of damage modes on laminate response was measured as stiffness reduction throughout the loading history where progressive development of damage was described and related to three stages of stiffness change. It is clear that the response of the three graphite epoxy laminates investigated is governed by a continuous process of damage initiation and growth during which existing damage modes interact to nucleate additional damage and/or new modes. This is especially true of matrix cracks, which are always identified as a damage mode but are often thought to be inconsequential. In the cases studied in this investigation, and in many other cases, matrix cracks are actually the source of other potentially critical damage modes.

DAMAGE MEASUREMENT USING RECENTLY DEVELOPED METHODS

Stress Wave Factor and Stiffness-Strength Relationships

Part of this subject matter was dealt with in Vol. 1 of this report. In that report it was shown that the measurement of specimen stiffness can be used as an excellent damage development parameter and can, in many instances, be interpreted in terms of the details of the microdamage that developed during fatigue loading. The present section will deal only with stiffness information and results which relate to other nondestructive testing activities. Specifically, we will focus on those results which are related to the characterization of composite materials by means of the ultrasonic stress wave factor (SWF). Present results indicate there is a close relationship between the nature of the results produced by stiffness change monitoring and by monitoring of the SWF.

Most nondestructive test techniques and methodologies presently in use have as their objective the detection and physical description of individual material imperfections such as matrix cracks, delaminations, porosity, fiber or matrix rich regions, etc. When such detection and description are obtained, it is still necessary to analytically establish the individual and collective significance of the defects that are identified in the context of consequent service performance and the success of this analysis must be validated. For the most part, the present investigators have taken a somewhat different approach to this problem. Several of the NDT techniques used and developed by the Materials Response Group produce information that is related to the total effect of the collective influence of the complex microdamage

states that are produced by fatigue loading of composite laminates. The measurement of changes in the tensor components of stiffness is a good example of this approach, as is the use of vibrothermography and the technique under present discussion, the stress wave factor (SWF).

The SWF is a method of utilizing ultrasound for nondestructively examining composite materials developed by Vary [5]. The technique employs a sending and a receiving ultrasonic transducer that are in contact with the same surface of the object being examined as illustrated in Fig. 4. Ultrasonic pulses generated by the sending transducer travel through the specimen and are received by another transducer a fixed distance away. The oscillations of the receiving transducer are counted above a selected threshold over a specific period of time. The stress wave factor then is stated as Eqn. (1)

$$SWF = ct(1/p) \quad (1)$$

where c is the number of oscillations, t is the period of time over which the counting is done, and $1/p$ is the repetition rate at which the sending transducer is emitting pulses. The SWF has many unique features, one of which is its sensitivity to the structural configuration of the object, i.e. lamina interfaces, lamina orientations, and boundaries which are manufactured into or created in the laminate. Because of this latter feature, it is possible to interrogate the material in specific directions which are of special interest, such as the direction of the applied load. One might expect regions which are poor conductors of information from one ultrasonic transducer to the other might also be "poor performers" relative to

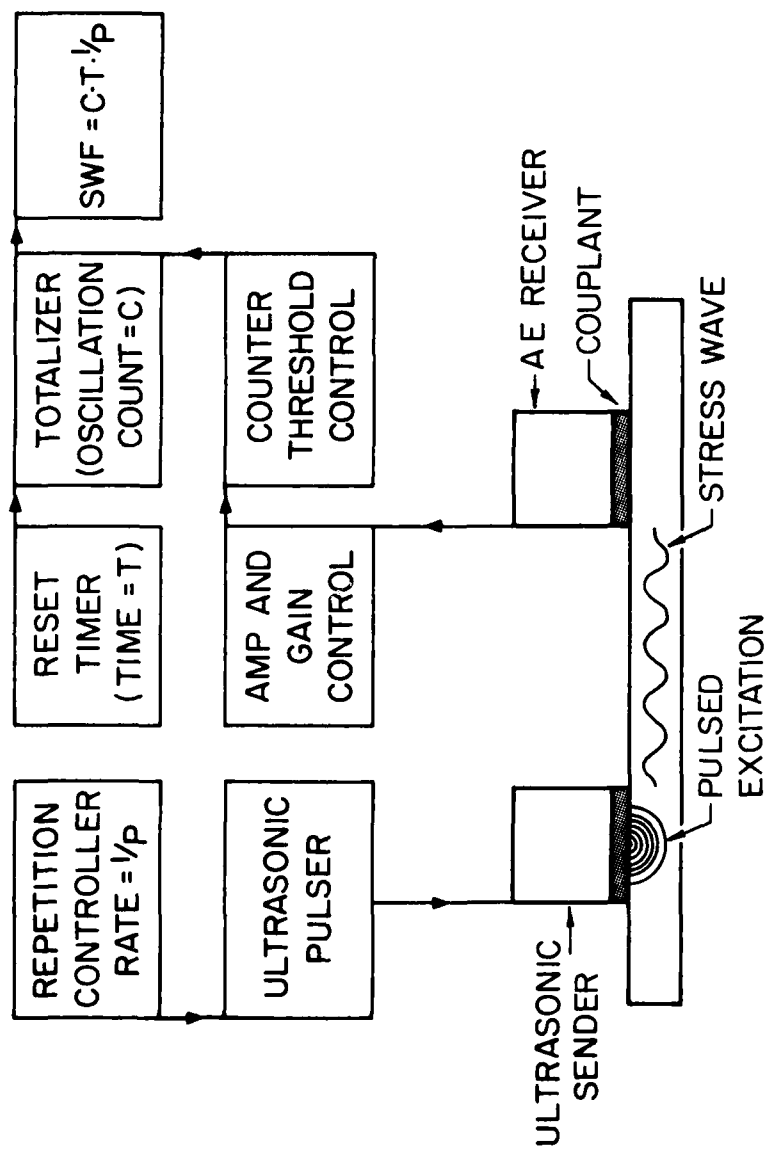


Fig. 4. Experimental arrangement for stress wave factor measurements.

neighboring regions. For instances in which a specimen is subjected to a homogeneous state of stress, a region having the lowest SWF might be expected to be the region where fracture would initiate.

A major consideration in the attempt to use this technique (or any other NDT method) is the degree to which the information and examination technique can be reproduced. In the Materials Response Laboratory we have made a special effort to characterize the parameters associated with the performance of this technique. It happens that the type and amount of couplant material, the transducer attachment method, the threshold level and period of counting, and the procedure for associating SWF values with a region of the material must all be carefully evaluated and considered [6]. Figure 5 displays the results of a SWF examination of a $[0,90_3]_S$ E-glass laminated composite. Transducers were positioned with a separation of 3.125 cm and were translated in increments of 0.63 cm to examine the entire specimen. SWF values were plotted in two ways: the solid line displays the SWF values for the increment at the point directly between the two transducers, while the broken line records the data that is the average of all SWF values obtained while a 0.63 cm region remains between the two transducers. (The latter procedure was developed to try to associate the SWF value with a small region or point of the specimen.) The schematic shown below the graph depicts the specimen and a grid indicates the various transducer positions. The shaded region indicates the position of the failure which resulted from quasi-static tensile loading of that specimen. It can be seen that the region of low SWF values correlates well with the failure location. Other experience obtained by investigators in the Materials Response Group are consistent

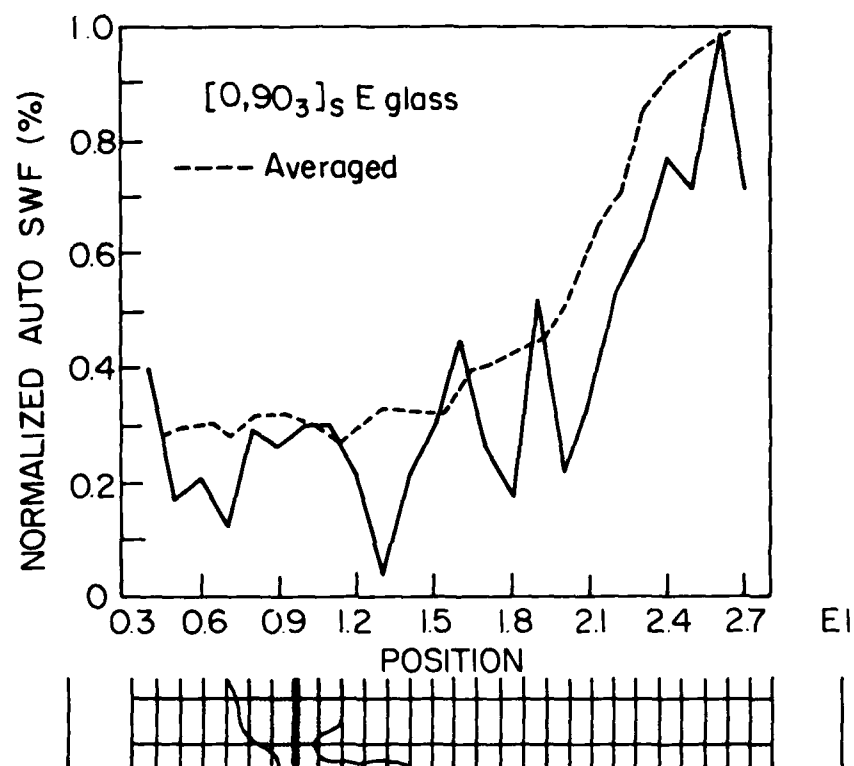


Fig. 5. Stress wave factor data compared to failure location (shaded) for a glass-epoxy specimen.

with this result [7]. These rather surprising results indicate that it may indeed be possible to locate the position at which a specimen will fail due to variations in internal integrity. It should be mentioned that these measurements were made on a specimen before deformation had occurred so that the correlations being made are correlations with the initial integrity of the laminates. This strongly suggests that, for a homogeneous applied stress state, the final location of fracture is associated with initial variations in the integrity of the material, a situation which may be interpreted in terms of the statistical variations in strength of various microvolumes of the material in general.

These results are especially interesting when viewed in the context of their relationship to stiffness changes. A number of experiments were performed to compare the stiffness of as-manufactured laminates to the measured SWF values. The technique of moiré interferometry was utilized to obtain the full-field in-plane axial displacement during quasi-static tensile loading. Since the interference patterns obtained may be interpreted as displacement, it is possible to determine the stiffness as a continuous function along the length of a straight sided coupon specimen subjected to tensile loading. Figure 6 is an example of the data produced by comparing SWF values with axial displacement measurements. All results were recorded at load values for which no detectable damage was present. It appears that these measurements are correlated in some way. The region over which both measurements were taken was identical. The exact nature of the correlation is material and laminate dependent [7].

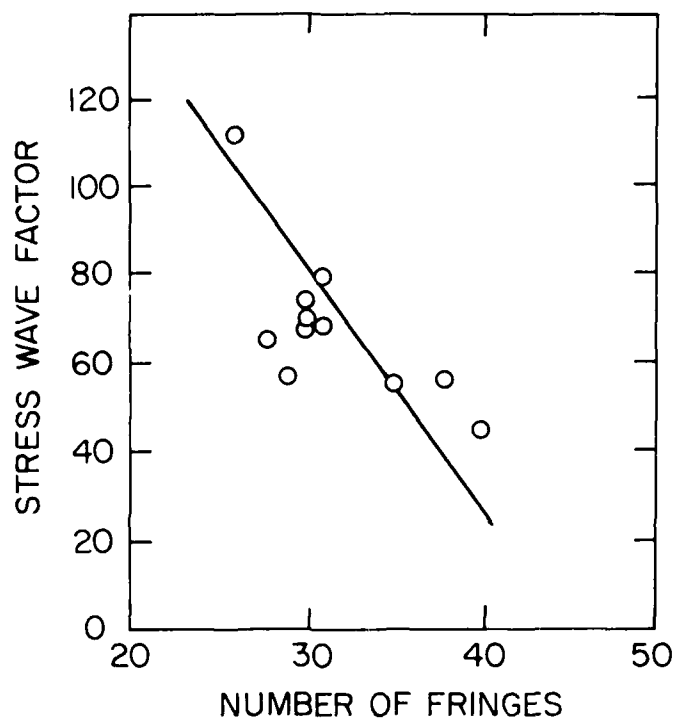


Fig. 6. Comparison of stress wave factor measurements with local stiffness implied from a moiré diffraction pattern.

Since the SWF is sensitive to the internal integrity and structure of composite materials, it would be expected that damage development during cyclic loading would also produce changes in the values recorded with such a technique. That is indeed the case as illustrated by Fig. 7. That figure presents data recorded from a graphite epoxy quasi-isotropic laminate during tension-tension cyclic loading with a maximum stress of 62 percent of the static ultimate strength of that laminate. The (secant) stiffness of the laminate was recorded continuously during the cycling with a computer-aided real-time data acquisition device. A monotonic change of stiffness is shown and was discussed in Vol. I of this report. In that discussion it was indicated that the stiffness changes are produced by three rather distinct types of activity which occur in three different regions over the life of the specimen. The SWF is also seen to demonstrate a monotonic decrease and also shows three rather distinct regions of behavior. The early stage of behavior up to about 15,000 cycles of loading can be thought of as an initiation stage where transverse cracks form and eventually saturate in density to create a "characteristic damage state" for matrix cracking as discussed earlier. In the second region, damage growth occurs usually at ply boundaries, induced and driven by the local stress fields at those boundaries that are created by the matrix cracks in the off-axis plies. The region over which that activity occurs can be seen to be between about 15,000 cycles and 50,000 cycles of loading. The final stage of damage involves delamination that initiates along the edge of the specimen and begins to grow into the interior and is seen to occur between about 50,000 and 70,000 cycles which was the fracture point of this test. The SWF factor is seen to be sensitive to these different

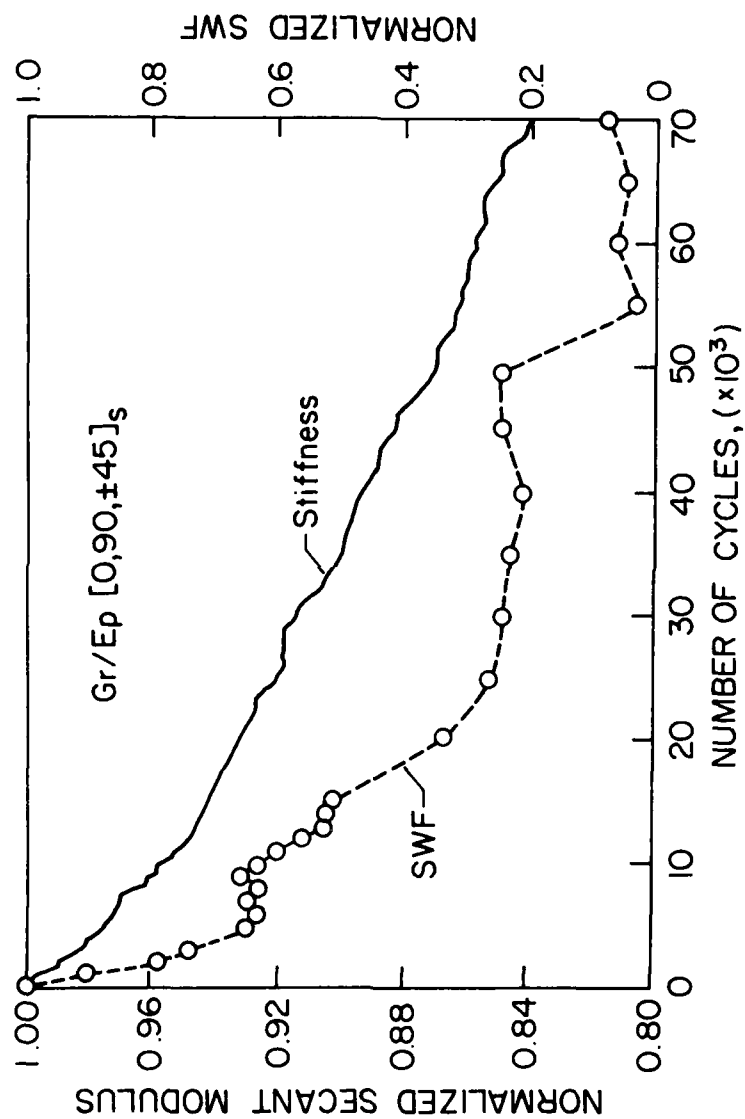


Fig. 7. Comparison of changes in SWF and axial stiffness of a fatigue loaded laminated composite specimen.

types of damage and shows the changes somewhat more explicitly in this case than the single component of stiffness that was measured in that test.

Another correlation with other nondestructive testing data is illustrated in Fig. 8. That test was conducted on a $[0,90]_{25}$ S-2 glass epoxy specimen at the mean stress indicated on the figure. The first part of the test data was truncated for purposes of illustration so that the initial region of damage development is not seen. A second and third stage of damage development (also discussed in Vol. I of this report) are evident. The third stage of damage development involves, in this case, longitudinal splitting which induces severe damage and eventual fracture of the specimen. The initiation of that damage stage and its progression are clearly indicated by the ultrasonic attenuation (specific damping), acoustic emission rate and secant modulus change. In fact, incipient fracture is clearly indicated by all three of these nondestructive test techniques. Of course, it is still not completely clear how to interpret the information obtained and the specific damping and acoustic emission data in terms of the specific details of the internal damage events that are occurring. While that is also true of the secant modulus results, a number of models have been developed which do relate those data to some of the mechanisms of damage development and to the degree of that development. By using several nondestructive test techniques which are sensitive in a discriminatory way to the details of damage development during cyclic loading of a laminate, it is possible to obtain more information than one could extract from any one of the single techniques alone, and more than one could create from a simple combination of information from those techniques.

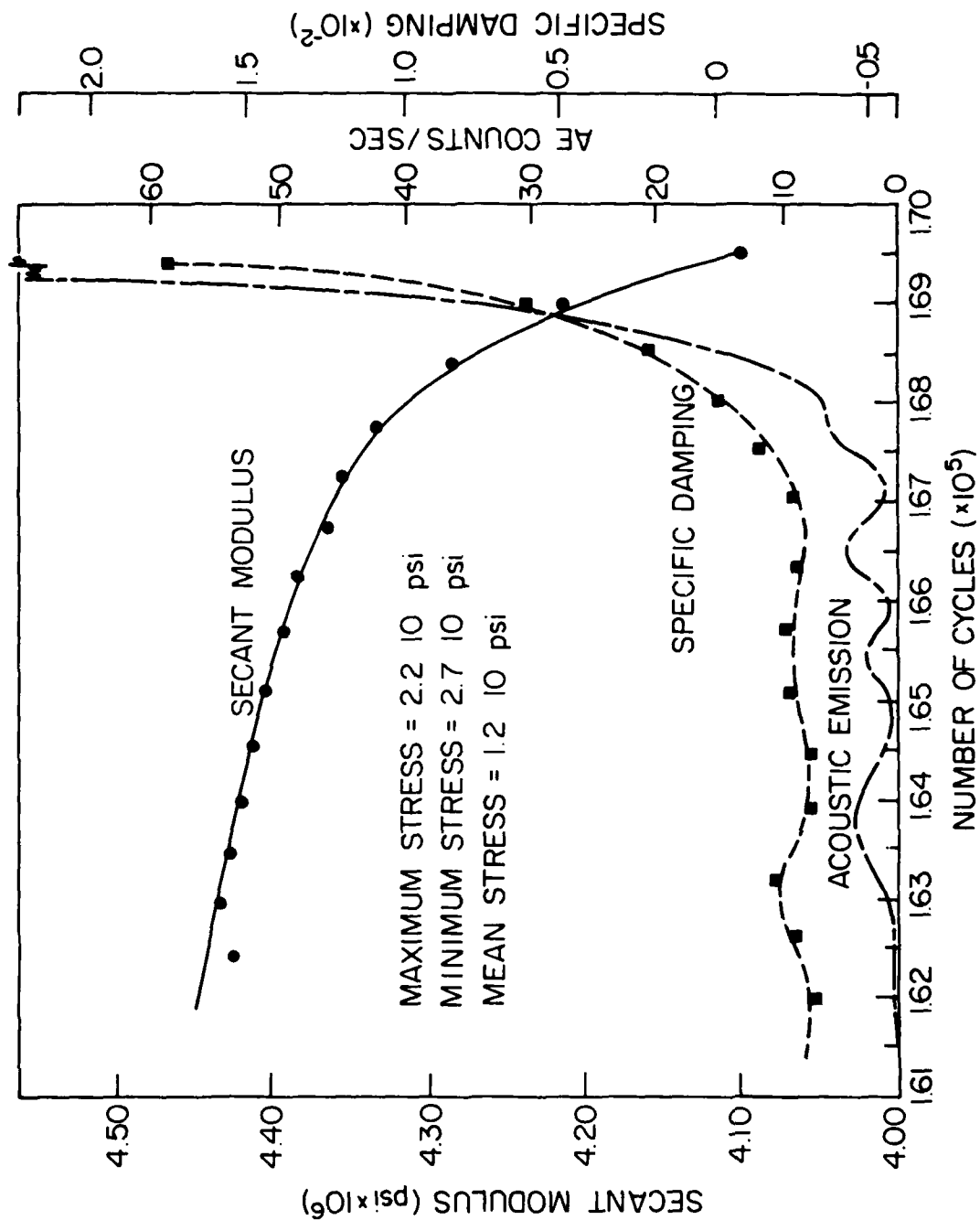


Fig. 8. Correlation of several types of nondestructive test data for a fatigue loaded $[0,90_2]_s$ glass-epoxy specimen.

Another interesting result regarding the use of nondestructive testing methods for the determination of life and residual strength is illustrated in Fig. 9. The dotted line in that figure is a recording of the continuous change of the secant modulus during the loading of a $[0,90]_{2s}$ S2 glass epoxy specimen with a maximum (tension-tension) amplitude of about 30 percent of its static ultimate strength which produced a lifetime of about 300,000 cycles. The initial strength of such a specimen is recorded as 150 ksi. Subsequent specimens were fatigue-loaded at the same level of stress and the tests were terminated at the numbers of cycles which correspond to the positions of the open circles on the abscissa. At that point, residual strength tests were run on those specimens and the data are indicated by the open symbols in Fig. 9. The scales of stiffness change and residual strength have been adjusted in order to emphasize the correlation between the residual strength and stiffness change for the specimens tested. It is clear that there is a strong correlation between the change in residual strength and the change in stiffness as these specimens are cyclically loaded. During the course of this investigation, a variety of other such correlations have been noted [1,3,8-16]. This kind of correlation strongly suggests that stiffness change can be used as an indicator of the consequences of the accumulation of damage and the amount of remaining strength in a specimen which has been fatigue-loaded. It also suggests that an understanding of the final fracture event should be closely related to an understanding of the exact manner in which the complex internal damage development process changes the residual stiffness of a composite laminate.

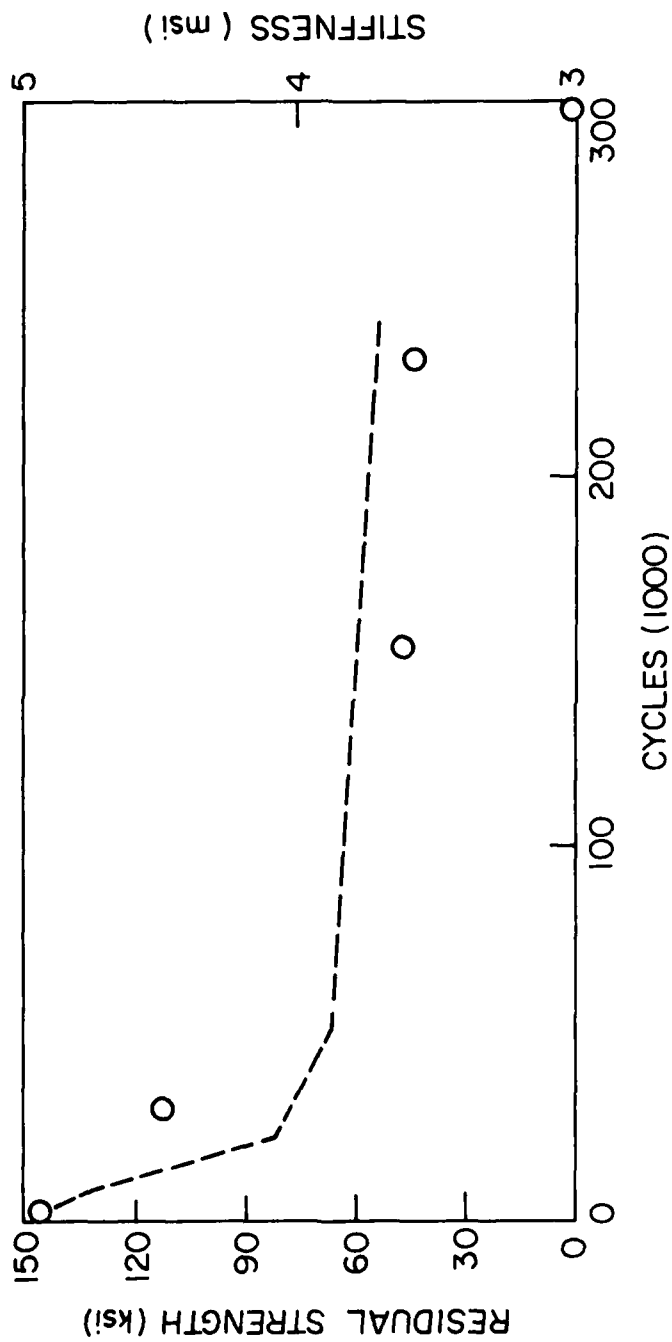


Fig. 9. Residual strength (open circles) and stiffness changes (dotted line) for a series of fatigue tests on glass-epoxy specimens.

Measurement of Inhomogeneous Micro-strain

One of the most fundamental findings of the present investigation is that matrix damage such as cracking and delamination cause significant local redistributions of stress. This local redistribution has been estimated by a variety of analytical methods as discussed in Vol. I of this report and in the publications generated during this investigation. The increase in local stress due to such redistribution can be large enough to cause reductions of the order of 30 percent in the residual strength of laminates, a reduction that is comparable in magnitude to the strength reductions observed in long-term fatigue loading.

While the general nature of these stress redistributions can be estimated from several approaches, the exact stress distributions must be obtained from three dimensional analyses and have not yet been determined in most cases. However, the most severe obstacle to progress in this area is the difficulty associated with attempts to measure the local nonuniform deformations caused by these stress redistributions. Unless such local changes can be measured the rational development of credible analytical representations will be hampered by the inability to validate correct approaches.

One of the high points of this investigation was the development of an experimental technique which is capable of measuring the nonuniform strains associated with local stress redistributions. While this technique is still under development, it has provided us with the first opportunity to establish by experiment the validity of analytical estimates of local nonuniform strains caused by matrix cracking and delamination. The technique is based on a moiré interferometry scheme

developed by D. Post which is capable of grating frequencies of up to 60,000 lines per inch, an increase of nearly an order of magnitude over comparable methods previously reported in the literature [17].

In our moiré interferometry apparatus, all of the elements shown in Fig. 10 except the specimen and its active grating, are attached to a mounting plate. A 5.0-mW helium-neon laser provides a beam of coherent monochromatic light. The laser beam is reflected by a front-surface mirror through a diverging lens. A spatial filter, consisting of a pinhole, is placed at the focal point to block out all light but that from the uniform intensity core of the beam, thus increasing the uniformity of the diverged beam. The diverging beam passes through a collimating lens, and is thus transformed into a parallel (and expanded) beam of light.

A silicone rubber grating with a frequency of 600 lines/mm is bonded to the specimen surface. The grating lines are perpendicular to the load direction. The collimated light is oriented with respect to the specimen so that the first-order diffraction of this light off the specimen grating is normal to the specimen surface. A portion of the beam is reflected by a front-surface mirror onto the grating so that both it and the direct beam, and thus their respective first diffraction orders, are symmetric about the normal to the specimen surface. When the grating is undeformed, the two first-order diffractions are parallel to each other and the phase difference is spatially constant. When the specimen (and grating) is deformed, the grating frequency is changed, which in turn alters the angle of diffraction of the two beams, and the phase difference between them varies spatially. The interference of the two first orders produces a series of light and dark fringes

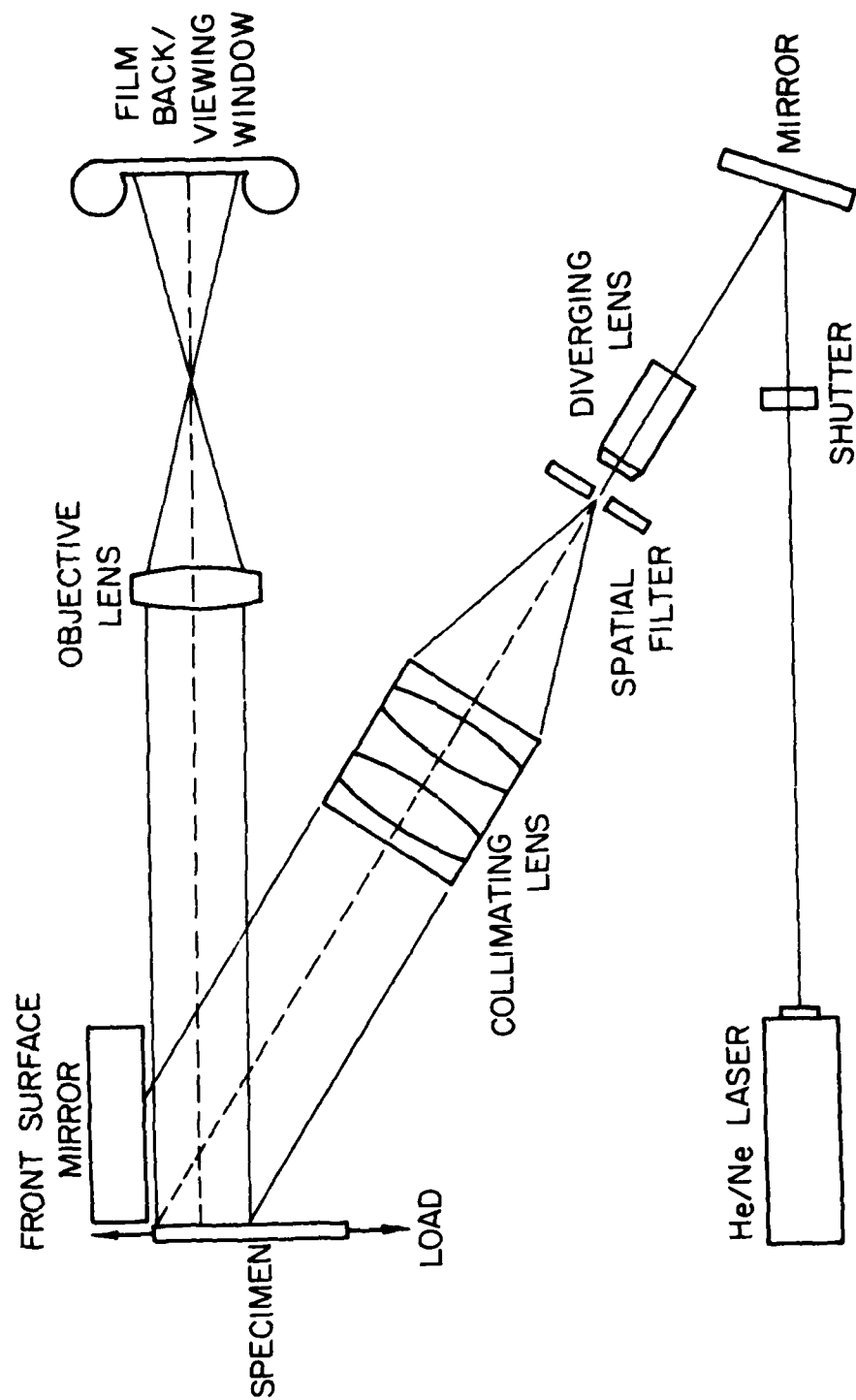


Fig. 10. Schematic of experimental arrangement for moiré diffraction investigations.

(constructive and destructive interference fringes) that correspond to contours of constant relative displacement (constant phase difference between the two diffracted beams) in the load direction. Because the interference pattern is formed by two first diffraction orders, the successive contour lines differ in displacement by $1/1200$ mm. (A more detailed discussion of moiré interferometry appears in Ref. [17]).

The optical system was mounted on an 89-kN (20-kip) MTS servohydraulic testing machine so that the displacement field in a tensile coupon could be examined in situ and photographed. One such fringe pattern, that of a $[0,90]_s$ glass/epoxy composite laminate loaded in axial tension, is presented in Fig. 11. The tensile load had caused cracks to form in the 90 deg plies transverse to the load axis. The fringe pattern clearly indicates that there is a gradient of longitudinal displacement in the 0 deg plies that results from the presence of these transverse cracks. The strain can be approximated by the discrete difference form of the derivative of the displacement using displacement values that correspond to the fringe pattern contours.

Another example of the utility of the moiré scheme for the measurement of inhomogeneous micro-strain is provided by our study of the redistribution of stresses caused by delamination. In order to investigate the effect of delamination on laminate response, a specimen with an artificial delamination was fabricated. Three pieces of T300/5208 graphite epoxy 254 mm long x 38.1 mm wide were bonded together using Miller-Stephenson type 907 two part epoxy adhesive. As shown in Fig. 12a, the two outer layers were $[0,90]_s$ material, while the central layer was $[+45,-45,-45,+45]_s$ material. A 50.8 mm long region on each of the mating surfaces was coated with vaseline before the adhesive was

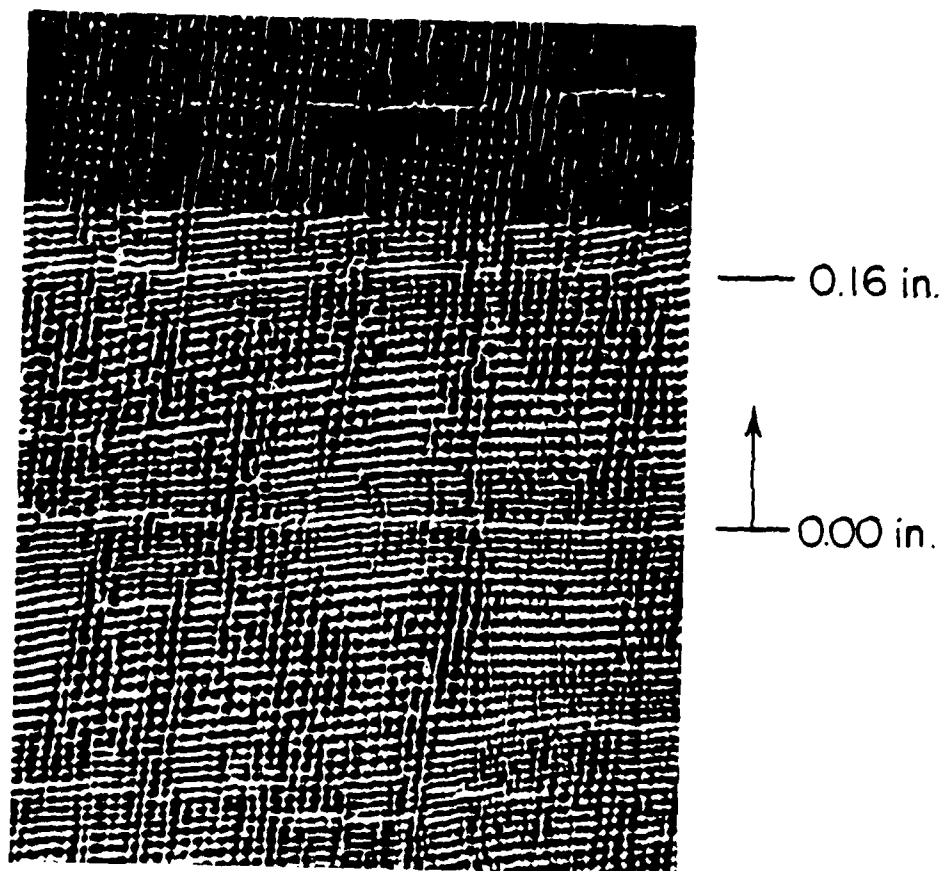
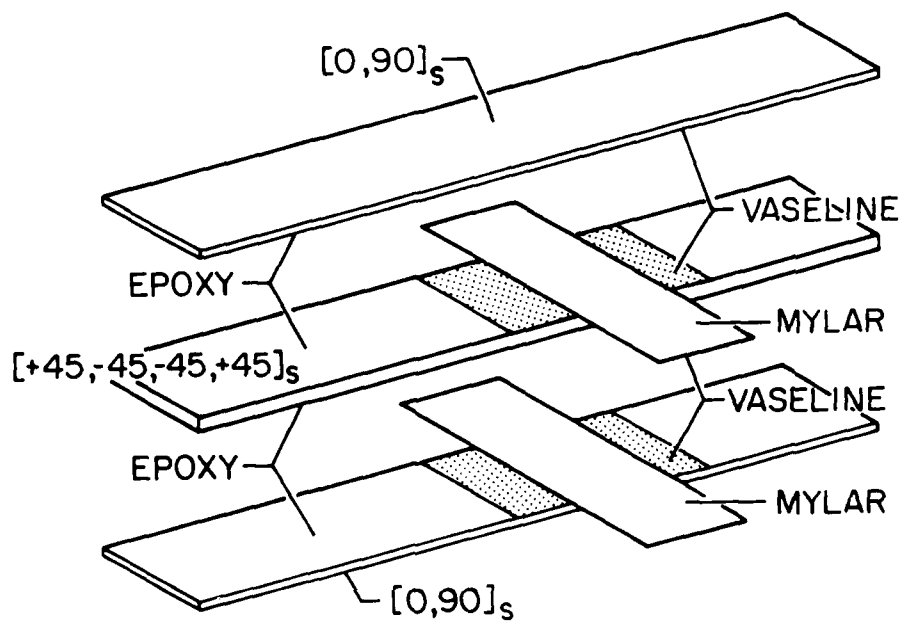
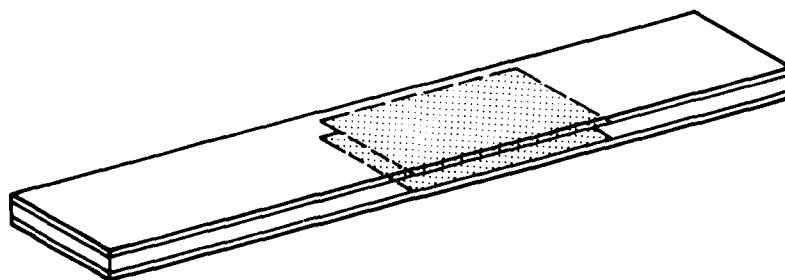


Fig. 11. Moiré diffraction pattern showing local increased strains in 0 deg. plies due to cracks in 90 deg. plies of a $[0,90_3]_S$ glass-epoxy specimen.



a)



b)

Fig. 12. Method of construction of controlled regions of delamination for stress redistribution studies.

applied. During assembly of the specimen, a 38.1 mm wide strip of mylar film was placed on the center of the vaseline coated region of each interface. After curing the adhesive, the mylar strips were removed, and the laminate was trimmed to 25.4 mm in width. The resulting specimen, shown in Fig. 12b, contained 50.8 mm long delaminations in the 0/45 interfaces which crossed the entire width of the specimen and were aligned along its length.

A moiré fringe pattern, Fig. 13, obtained from this specimen indicates how the delamination influences material response. Again, each fringe is a contour of relative axial displacement. In the undamaged region, the fringes are straight and uniformly spaced. In the delaminated region the fringes are curved, and are also closer together than those in the undamaged region. The difference in fringe density indicates that the axial strain is greater in the delaminated region. This difference in strain arises because the three layers are not constrained to have the same transverse and in-plane shear strains in the delaminated region. The Poisson's ratio mismatch between the two types of layers causes the distributions of stresses in the two regions to differ. This also explains why the moiré fringes are curved in the delaminated region. The transverse constraint relaxation takes place more readily near the specimen edge, and thus the transition from undamaged to delaminated response occurs over a shorter distance. Away from the edge near the delamination front, the delaminated layers are still somewhat constrained by the surrounding material. A simple stress analysis using laminate theory can be performed to estimate the effect of delamination on internal stresses. In this analysis, the three layers in the delaminated region are required to have equivalent

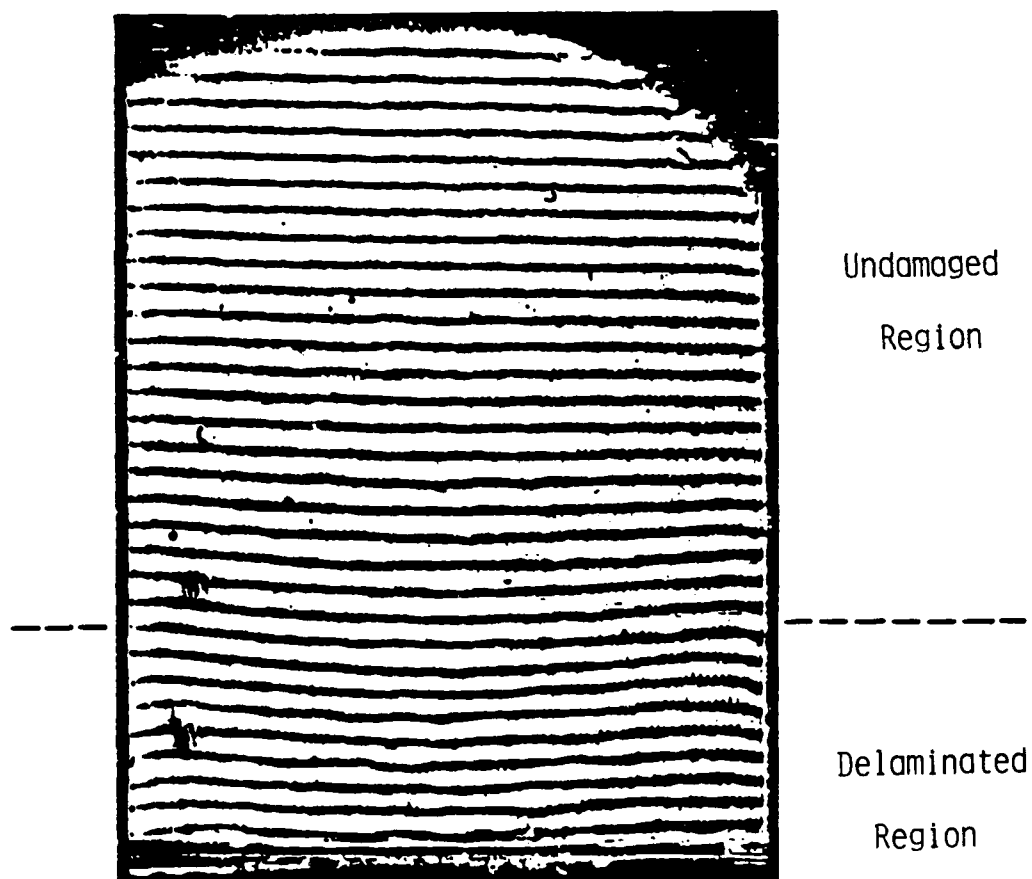


Figure 13. Moiré fringe pattern taken from specimen SC-1 spanning both undamaged and delaminated regions.

longitudinal strain, but no restrictions are imposed on the transverse and shear strains. Equilibrium requires that the delaminated and undelaminated regions are subjected to the same total load. The predictions of in-plane stresses in each ply of both the delaminated and undamaged regions are presented in Table I. Note that σ_x in the zero degree plies is larger in the delaminated region, as indicated by the moiré pattern. Using a one in. gage length clip-on type extensometer, local axial strain response was monitored in both the undamaged and delaminated regions. This data is presented in Fig. 14. (Load was chosen instead of stress because the material cross-sections in the delaminated and undamaged regions differ by 2 thicknesses of epoxy adhesive. However, the adhesive is relatively compliant so this discrepancy should not significantly affect the results). The reduction of axial stiffness due to the delamination was observed to be 14.3 percent. The simple analysis discussed above predicts a 12.7 percent reduction in stiffness.

It is true that the delaminations in the specimen discussed above can hardly be considered local because they cover a large portion of the adhesive interfaces. Local delaminations appear to be more constrained by the surrounding material. However, interaction of other damage events with the local delaminations have thus far been ignored. Quasi-static tensile tests were performed on $[0,90,\pm45]_5$ graphite epoxy specimens which had aligned delaminations at both 0/90 interfaces. These delaminations were produced by taping together two 25.4 mm wide strips of mylar fiber stacked atop one another, and placing one such delamination at each 0-90 interface during the layup of the laminate prior to curing. During tensile loading, axial strain was monitored via

Table I. Comparison of in-plane stresses predicted via laminate analysis for a $[0,90,90,0,+45,-45,-45,+45]_s$ graphite epoxy laminate (lamina properties: $E_1 = 141.6$ GPa, $E_2 = 10.2$ GPa, $\nu_{12} = 0.305$, $G_{12} = 6.00$ GPa, $N_x = 113.0$ kN-mm) with and without delamination at the 0-45 interfaces.

Ply	Damage Condition	σ_x (MPa)	σ_y (MPa)	τ_{xy} (MPa)
0	undamaged	399.4	0.1	0.0
	delaminated	459.1	8.8	0.0
90	undamaged	26.3	-112.6	0.0
	delaminated	32.7	-8.8	0.0
+45	undamaged	100.3	56.2	65.1
	delaminated	67.2	0.0	27.9
-45	undamaged	100.3	56.2	-65.1
	delaminated	67.2	0.0	-27.9

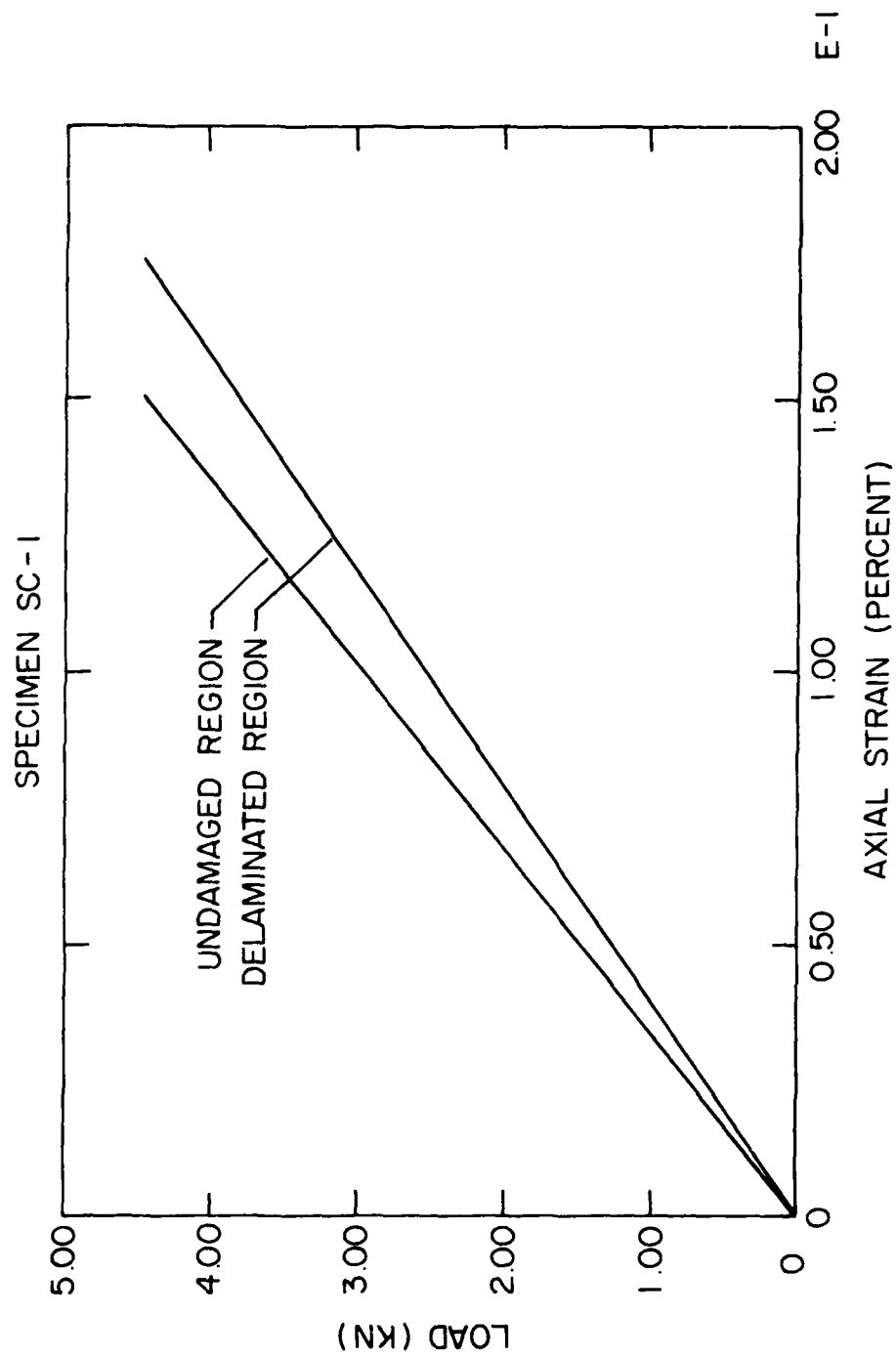


Fig. 14. Comparison of specimen effective stiffness in delaminated and undelaminated regions.

both a 25.4 mm gage length clip gage that spanned just the delaminated zone, and a 50.8 mm clip gage that spanned both the delaminated region and undamaged material. While no measurable difference in stiffness was detected (or predicted) the average reduction in tensile strength from that observed in specimens without delaminations was 25.4 percent. This is nearly the reduction in strength that would be expected if the interior plies carried no load. It is possible that other damage is coupling with the delamination and mechanically separating the zero degree plies from the interior plies.

FIBER FRACTURE

In Vol. I of this report, and in the eleven other publications associated with this research contract, we have focused rather heavily on matrix damage as the primary constituent of fatigue damage development in composite laminates. Matrix cracking and delamination (both internal and edge delamination) has been shown to cause stress redistribution and changes in internal geometry which can greatly influence the residual properties of a composite laminate. In addition, most of the "growth" that occurs during damage development under fatigue loading consists of the growth of matrix damage such as crack coupling, and delamination.

However, the failure of fiber-dominated composite laminates must result from the ultimate failure of the zero degree plies. Hence, the ultimate strength of such a laminate under either quasi-static or fatigue loading is controlled by the condition of the fibers and the stress state created by microdamage in both the fibers and the matrix materials. As we have discussed in Vol. I of this report, matrix damage serves primarily to vary the state of internal stress in the neighborhood of microdamage events. Fiber fractures can be regarded as material degradation in a more basic sense.

As we noted in Vol. I of this report (and in our earlier publications) the association between fiber fractures and matrix cracking in the off-axis plies is a nearly exclusive one in the sense that fiber fractures in the zero degree plies of all of the laminates examined (including stacking sequences of $[0,90_2]_s$, $[0,\pm45]_s$, and $[0,90,\pm45]_s$) were observed to occur in periodic arrays which were

exclusively associated with matrix cracks in adjacent plies and, conversely, virtually no fiber fractures were observed in regions between those associated with such cracks. Fiber failures continued to occur in these locations throughout the life of the material. The rate of fiber fracture seems to be very much greater in the early part of the life (up to about one-third of the total life span) than it is throughout the remainder of the loading history, even for load amplitude levels which are of the order of 50 or 60 percent of the static ultimate strength. Hence, the initiation of fiber failures in the neighborhood of matrix cracks can be thought of as the second chronological internal damage event.

As we mentioned in our earlier discussions, the number of fibers that fail during cyclic loading to fracture is generally much greater than the number of fibers that fail during quasi-static loading to fracture, generally four times to ten times as large. Stated in another way, it can be said that a relatively low stress amplitude applied during cyclic loading over a large number of cycles produces significantly larger numbers of fiber fractures than does a comparatively larger stress level applied during quasi-static loading. In a sense, this observation is logical since the (residual) strength of a fatigue loaded composite specimen must be reduced to the level of load application if failure is to occur after a large number of cycles of loading have been applied. It is reasonable to assume that this strength reduction occurs by degradation of the fibers in the plies in addition to the stress redistribution that occurs because of matrix damage during that process. However, it should be noted that a great majority of the fiber fractures that are observed during fatigue loading

occur in the early part of the test. Two important conclusions can be drawn from these combined observations. First, we have produced no evidence (and we are aware of none) that indicates that the residual strength of the fatigue loaded composite laminate specimens of the type we have examined is directly proportional to the total number of single fiber breaks that can be counted in the interior of the specimen as a function of time or cycles of loading. And second, there is a continuous process which is responsible for the development of fiber fractures that appears to be initiated and influenced by matrix cracks, but which also involves some growth process which results in the creation of some damage state that is critical in the sense that it is the immediate precursor of incipient fracture of the total specimen. These two points will be developed somewhat further below.

One way to illustrate the existence and nature of a fiber fracture process is to consider the information given in Figs. 15 and 16. The data in those figures was developed from a destructive, microscopic technique developed by Freeman [18]. In this method, the specimen is heated to a temperature sufficient to partially pyrolyze the resin matrix. The interlaminar bond strength is thereby diminished to the extent that the individual plies of the laminate can be separated. The heating was accomplished in an electric tube oven in an argon gas environment. Sufficient resin material remains after pyrolysis to hold the plies together if they are handled carefully. Introduction of an enhancing agent along the edges of a specimen prior to the deply procedure served to enhance the internal regions of damage for ease in visual identification, much in the manner of X-ray image enhancement by opaque material. The separated plies were examined by both light and

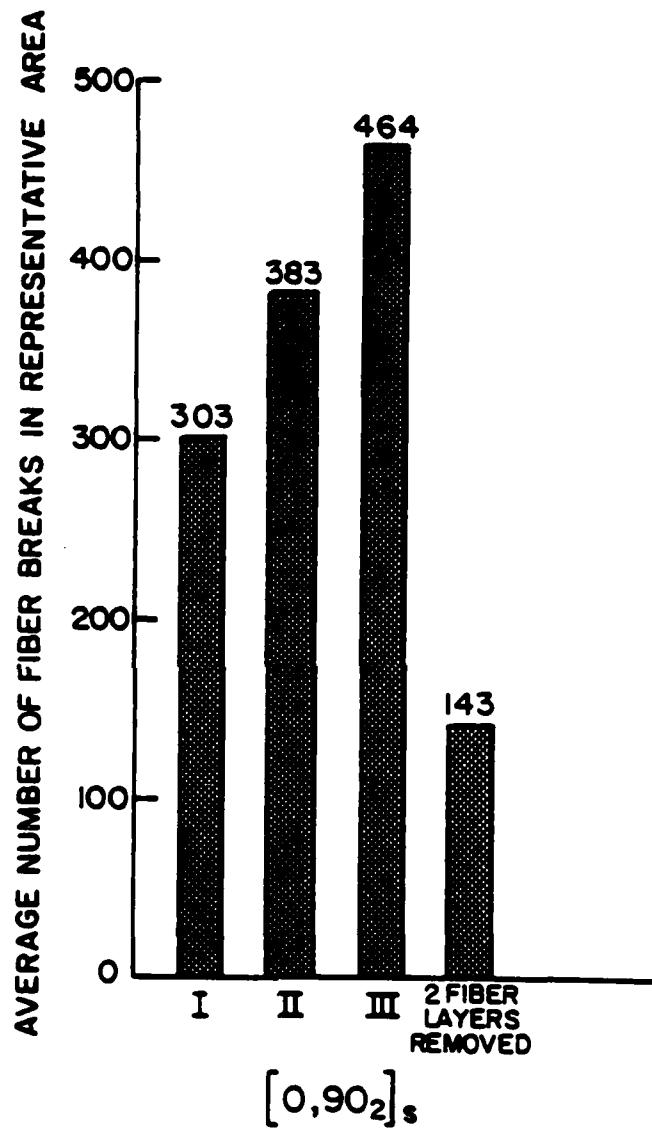


Figure 15. Average number of fibers broken in a fixed area of viewing at about one-third, two-thirds, and nearly one full lifetime of cyclic loading for a graphite epoxy laminate.

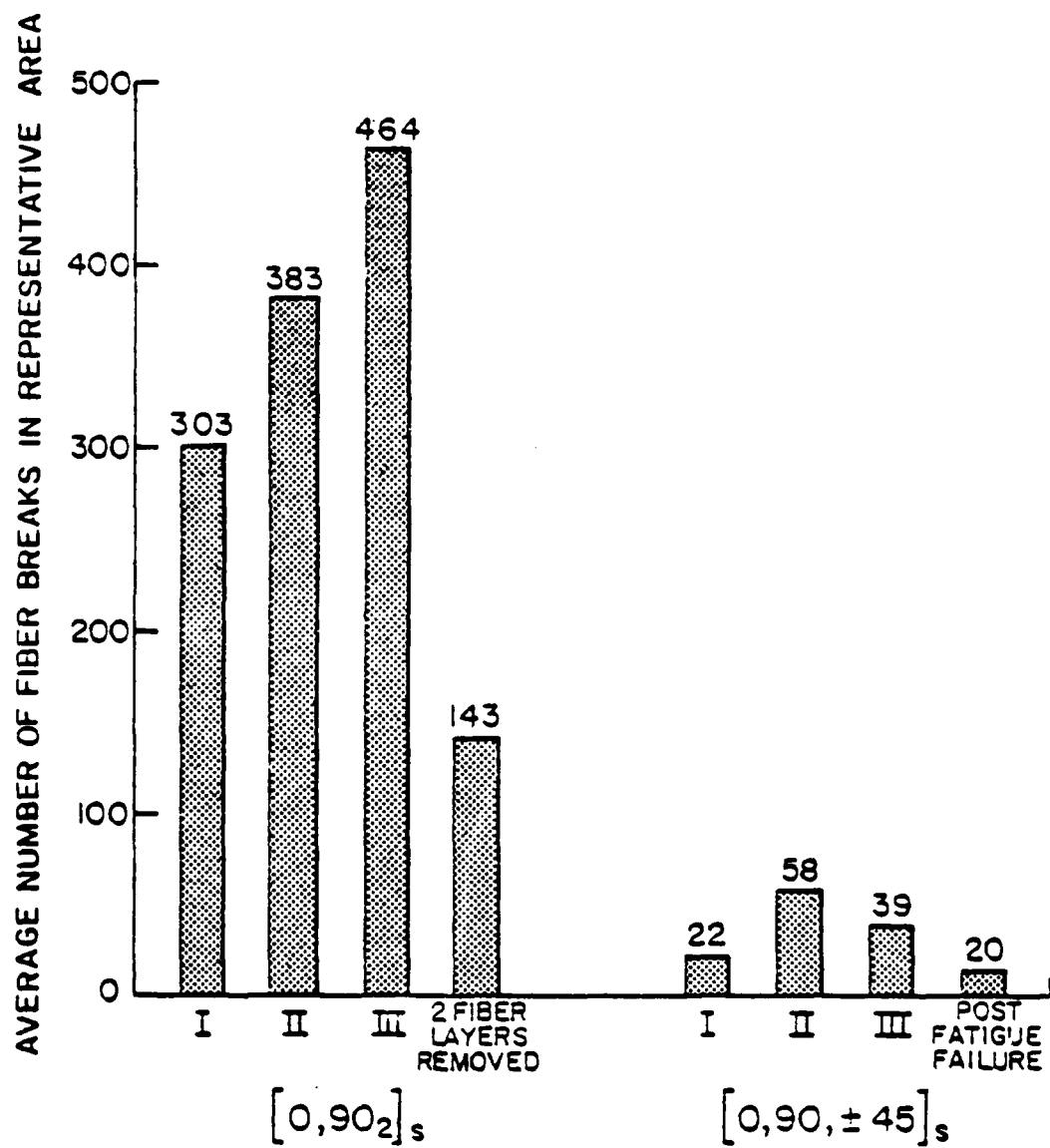


Figure 16. Total Fiber Fractures in $[0,90,\pm 45]_s$ Laminates.

electron microscopy. Coupons were cut from the deplied laminae for SEM examination so that the details of fiber fracture could be studied. Working magnifications for the study of patterns of fiber breaks was 200 to 400X; to study the details of individual fiber fractures, magnifications of from 1600 to 2000 were required.

The zero degree plies of fatigue damaged $[0,90_2]_S$ and $[0,90,\pm 45]_S$ laminates were examined for evidence of interior fiber fractures. Coupons measuring approximately 6 mm square were cut from each of the deplied load-bearing laminae and examined in the scanning electron microscope. Examinations were conducted at roughly one-third, two-thirds, and near the end (or following fracture) during a test. In general, several hundred samples of fiber fracture patterns were investigated for each of the observations in Figs. 15 and 16. In addition to counting the number of single fibers that were broken, it was decided to also record the number of fibers that were broken in proximity to one another. It was necessary to choose an arbitrary distance from a given fracture within which an additional fiber fracture was considered to be related to the first one. While the choice of such a distance will certainly influence the absolute value of the results obtained, the nature of the results was found to be unaffected by this choice. In the present case, it was considered that any fiber fracture which was located within five fiber diameters of another fiber fracture was associated with that fracture event and was considered to be a doublet; three such fiber fractures located within five fiber diameters of each other were regarded as a triplet; four or more such fiber fractures within five fiber diameters of each other were regarded as a

multiplet. A sample of such observations are included in Figs. 15 and 16.

In Fig. 15 it is seen that for the $[0,90_2]_5$ laminate under fatigue loading, the number of multiple fiber fractures increases as a function of the number of applied cycles of loading. (The last column of data in Fig. 15 was developed by removing two fiber layers from the zero degree ply under observation and making a recount of the fiber fractures observed.) The I, II, and III indicate stages 1, 2, and 3 of the test as discussed in earlier reports and can be regarded, for the purpose of our present discussion, as roughly one-third, two-thirds, and the final third of test time. For the data that was obtained just prior to fracture of the specimen, the distribution of data obtained was 78 percent singlets, 17 percent doublets, 3 percent triplets, and 2 percent higher order multiplets for the test shown. The highest order multiplet observed was 8. For comparison purposes it can be noted that the same type of laminate was observed near static failure and a distribution having 90 percent singlets, 8 percent doublets, and only 1 percent each of triplets and higher order multiplets was observed. In that instance for quasi-static loading the highest order multiplet observed was 4. Hence, not only is the number of total fiber fractures and order of magnitude greater for fatigue loading than for quasi-static loading, the number of fibers that break in close proximity to one another is also much larger for cyclic loading than for the quasi-static case. Hence, it is clear that there is some process of fiber fracture development during the cyclic loading experience, a process that seems to involve the development of fiber fractures which are in the neighborhood of fibers that break at an earlier time. Figure 16 shows an interesting

comparison between the quasi-isotropic laminate and the $[0,90_2]_s$ laminate discussed in Fig. 15. For the quasi-isotropic case at incipient failure the distribution of fiber failures consists of 85 percent singlets, 7 percent doublets, and 8 percent triplets. The highest order multiplet observed was 3. The difference between the number of fibers that fractured during cyclic loading of the quasi-isotropic laminate and the quasi-static loading case for that laminate was smaller than for the previous laminate stacking sequence; approximately 4 times the number of fibers that failed in the quasi-static case were observed in the fatigue case. In that context it should be mentioned that the global zero degree ply stress at laminate failure was 22 percent higher for quasi-static loading than for the fatigue data developed and shown in Fig. 15, while the difference was only 7 percent between the quasi-static and fatigue failure amplitudes for the data representing the quasi-isotropic laminate in Fig. 16.

The second major observation that we wish to develop here involves the question of an incipient specimen fracture state that is defined by fiber fracture and the adjacent matrix damage. In Vol. I of this report (and in other publications which appeared earlier) we have emphasized, with some excitement, that the internal stress redistribution that can occur when delamination of various plies of the laminate occurs can be sufficiently large so as to increase the stress in the load direction in the zero degree plies by an amount of the order of 20 to 30 percent, an amount which can account for the large strength reductions that are necessary to explain the fracture of a fatigue loaded specimen which is cycled at a tensile amplitude of 70 percent of the static ultimate

strength. Delaminations have been observed in the interior of specimens for the first time during the course of this investigation.

However, there is strong evidence that internal stress redistribution alone does not generally reduce the residual strength of the laminates to the level of the applied fatigue loads in order to cause fracture. Delaminations (at the edge or in the interior) are generally not sufficiently large to cause the total amount of internal stress redistribution discussed above, and a process of fiber fracture is also observed as described earlier. Since the rate of fiber fractures appears to be large at the beginning and end of a given fatigue life, and is generally considerably smaller during a period of what might be called "stable growth" in the middle of such a period, and especially in view of the information regarding multiple fiber fractures presented in Figs. 15 and 16 and discussed above, it appears that a philosophy of specimen fracture initiation based on simple overload of the zero degree plies as internal stresses are redistributed by matrix damage and as the total cross-section of the zero degree plies is reduced by fiber fracture is not appropriate. Rather, the data suggests that the internal incipient fracture state is created by the progressive localization of damage to form a region of critically high local stress associated with groups of fiber failures which occur in close proximity to one another and contributed to by the stress state associated with the other damage in that region. Such an observation is consistent, for example, with the fact that the highest order multiplet observed in the $[0,90_2]_5$ laminate for which the zero degree ply stress at laminate failure under fatigue loading was 22 percent lower than for the corresponding quasi-static case was 8, while the highest order multiplet

observed for the $[0,90,\pm45]_5$ laminate for which the corresponding difference in the zero degree ply stress was only 7 percent was 4. In a simplistic sense, one could say that a longer "crack" was required to fracture the zero degree plies in a specimen for which the component of applied stress in those plies was low, and a correspondingly shorter "crack" was required to fracture the zero degree plies in a laminate for which the component of applied stress in those plies was larger. While such an observation is by no means a conclusion, we know of no evidence to the contrary.

Since the fracture event itself in composite laminates constructed from high modulus fibers is a highly dynamic energy redistribution process, the precise details of that process have not been experimentally observed. Therefore, it is impossible to say with certainty exactly how specimen fracture begins, precisely what state of damage and state of stress is responsible for its initiation, and what fracture mechanism is involved. However, we believe the observations described above bring us very close to the answers to those questions. Additional certainty will require additional investigation.

References

1. Reifsnider, K. L., Henneke, E. G., Stinchcomb, W. W. and Duke, J. C., "Damage Mechanics and NDT of Composite Laminates," Proc. of Int'l. Union of Theoretical and Applied Mechanics (IUTAM), Mechanics of Composite Materials, Blacksburg, VA, Pergamon Press, 1983.
2. Sendekyj, G. P., "NDE Techniques for Composite Laminates", AGARD Specialists' Meeting on Characterization, Analysis, and Significance of Defects in Composite Materials, London, Apr. 1983.
3. Jamison, R. D. and Reifsnider, K. L., "Advanced Fatigue Damage Development in Graphite Epoxy Laminates," Interim Report to AF Wright Aeronautical Laboratories, AFWAL TR-82-3103 (Dec. 1982).
4. Schulte, K. and Stinchcomb, W. W., "Damage Development Near the Edges of a Composite Specimen During Quasistatic and Fatigue Loading," submitted to Composites Technology Review.
5. Vary, A. and Bowles, K. J., "An Ultrasonic-acoustic Technique for Nondestructive Evaluation of Fiber Composite Quality", Polymer Engrg. Sc. 19 (1979) pp. 373-377.
6. Henneke, E. G., II, Duke, J. C., Jr., Stinchcomb, W. W., Govada, A. and Lemascon, A., "A Study of the Stress Wave Factor Technique for the Characterization of Composite Materials", Interim Report of NASA NaG 3-172 (June 1982).
7. Duke, J. C., Jr., Henneke, E. G., II, Stinchcomb, W. W. and Reifsnider, K. L., "Characterization of Composite Materials by Means of the Ultrasonic Stress Wave Factor", Int'l. Conf. on Composite Structures, Sept. 14-16, 1983, Paisley College of Technology, Scotland.
8. Jamison, R. D., Schulte, K., Reifsnider, K. L. and Stinchcomb, W. W., "Characterization and Analysis of Damage Mechanics in Fatigue of Graphite Epoxy Laminates," Proc. of Symp. on Effects of Defects in Composites, Am. Soc. for Testing and Materials, 14 Dec. 1982, San Francisco.
9. Highsmith, A. L., Stinchcomb, W. W. and Reifsnider, K. L., "The Effect of Fatigue-Induced Defects on the Residual Response of Composite Laminates," Proc. of Symp. on Effects of Defects in Composites, Am. Soc. for Testing and Materials, 14 Dec. 1982, San Francisco.
10. Highsmith, A. L. and Reifsnider, K. L., "Measurement of Nonuniform Microstrain in Composite Laminates," Composites Technology Review, (Spring 1982) p. 20.

11. Reifsnider, K. L., Stinchcomb, W. W., "Stress Redistribution in Composite Laminates," Composites Technology Review (Spring 1981), p. 32.
12. Jamison, R. D., Highsmith, A. L. and Reifsnider, K. L., "Strain Field Response of 0° Glass Epoxy Composites Under Tension," Composites Technology Review (Winter 1981), p. 158.
13. Reifsnider, K. L. and Jamison, R. D., "Fracture of Fatigue-Loaded Composite Laminates," Int'l J. of Fatigue, 4, no. 4 (1982) pp. 187-198.
14. Highsmith, A. L. and Reifsnider, K. L., "Stiffness-Reduction Mechanisms in Composite Laminates," Damage in Composite Materials, Special Technical Publication 775, K. L. Reifsnider, Ed., American Society for Testing and Materials (1982) pp. 40-62.
15. Stinchcomb, W. W. and Reifsnider, K. L., "Fatigue Damage Mechanisms in Composite Materials: A Review," Fatigue Mechanisms, ASTM STP 675, J. T. Fong, Ed. (1979).
16. Reifsnider, K. L. and Jamison, R. D., "Fracture of Fatigue-Loaded Composite Laminates," Int'l. J. of Fatigue (Oct. 1982) pp. 187-197.
17. Mechanics of Nondestructive Testing, W. W. Stinchcomb, Ed., Plenum Press, New York, (1980).
18. Freeman, S. M., "Characterization of Lamina and Interlaminar Damage in Graphite-Epoxy Laminates by the Depty Technique", STP 787, American Society for Testing and Materials, (1982).